JBC Papers in Press. Published on April 4, 2019 as Manuscript RA118.005772
The latest version is at http://www.jbc.org/cgi/doi/10.1074/jbc.RA118.005772

Dihydronicotinamide riboside is a potent NAD$^+$ concentration enhancer in vitro and in vivo

Yue Yang[1], Farheen Sultana Mohammed[1], Ning Zhang[1] Anthony A. Sauve[1]

From the [1]Department of Pharmacology, Weill Cornell Medical College, New York, NY 10065

Running title: *NRH increases NAD$^+$ concentrations in cells and tissues*

To whom correspondence should be addressed: Anthony A. Sauve 212-746-6224, aas2004@med.cornell.edu

Keywords: NAD$^+$, NRH, nicotinamide riboside, dihydronicotinamide riboside, NAD$^+$ precursor

ABSTRACT

Interest in pharmacological agents capable of increasing cellular NAD$^+$ concentrations has stimulated investigations of nicotinamide riboside (NR) and nicotinamide mononucleotide (NMN). NR and NMN require large dosages for effect. Herein we describe synthesis of dihydronicotinamide riboside (NRH) and the discovery that NRH is a potent NAD$^+$ concentration enhancing agent, which acts within as little as 1 hr after administration to mammalian cells to increase NAD$^+$ concentrations by 2.5-10 fold over control values. Comparisons to NR and NMN show that in every instance NRH provides greater NAD$^+$ increases at equivalent concentrations. NRH also provides substantial NAD$^+$ increases in tissues when administered by intraperitoneal injection to C57BL/6J mice. NRH substantially increases NAD$^+$/NADH ratio in cultured cells and in liver, and no induction of apoptotic markers or significant increases in lactate levels in cells. Cells treated with NRH are resistant to cell death caused by NAD$^+$-depleting genotoxins such as hydrogen peroxide and methylmethane sulfonate. Studies to identify its biochemical mechanism of action showed that it does not inhibit NAD$^+$ consumption suggesting it acts as a biochemical precursor to NAD$^+$. Cell lysates possess an ATP-dependent kinase activity which efficiently converts NRH to the compound NMNH, but independent of Nrk1 or Nrk2. These studies identify a putative new metabolic pathway to NAD$^+$, and a potent pharmacologic agent for NAD$^+$ concentration enhancement in cells and tissues.

NAD$^+$ metabolism is largely comprised of biosynthetic, redox-active and "NAD$^+$-consuming" pathways (1,2). In biosynthetic pathways NAD$^+$ is made from different NAD$^+$ precursors. In redox active pathways NAD$^+$ is used to conduct hydride equivalents between reductants and oxidants. In NAD$^+$-consuming pathways, NAD$^+$ is consumed via enzymes that transfer the ADPR moiety to cellular nucleophiles (3,4). Reactions in each group are plentiful in cells making NAD$^+$ one of the most versatile of cellular metabolites. NAD$^+$ is required in abundant amounts, existing at concentrations of 100-500 μM in most mammalian cells and tissues (See Table 1 for examples)(5). NAD$^+$ metabolism has become a topic of renewed interest in recent years (6), notably focused upon the involvement of ADPR transfer/sirtuin deacylation reactions in mediating key cellular processes (7), such as DNA repair (8), metabolic adjustment (8), apoptosis (5), cell survival (6), stem cell fitness (6,9), and even lifespan regulation (9-11).

The substrate role of NAD$^+$ for key signaling enzymes has sparked investigations to determine whether increased NAD$^+$ concentrations provide an impetus for cellular changes. Of interest are genetic or pharmacologic interventions that can significantly alter NAD$^+$ concentrations, probing for downstream effects mediated by ADPribosyltransferases/sirtuins. This work has provided evidence that increased NAD$^+$ concentrations drive signaling programs leading to key biochemical processes such as enhanced mitochondrial biogenesis (12), protection against fatty acid induced liver disease (13), improved

exercise performance (14), and reduced neurodegeneration (15,16) in a variety of animal models. In turn, these results have turned attention to nicotinamide riboside (NR)(17-19) and nicotinamide mono-nucleotide (NMN) (18,19) as possible NAD$^+$ precursors, with findings that these agents are promising for raising cellular and tissue NAD$^+$ concentrations. Very recently a number of clinical studies of these agents in humans have been published (20-22), confirming their activities as NAD$^+$ concentration boosters in humans, and setting the stage for further development as human therapeutics (1,6).

There are limitations of the current set of NAD$^+$ concentration enhancers, including maximal reported cellular effects for NAD$^+$ enhancement of 270 percent (17), and requirements of high doses to achieve beneficial effects in animal models of disease with reported doses typically 250-1000 mg/kg in mice (14,23,24). These limitations stimulated our laboratory to investigate other chemical structures related to NR and NMN as possible NAD$^+$ precursors. Of interest to us was dihydronicotinamide riboside (NRH) which has never been investigated as a precursor in NAD$^+$ metabolism, to our knowledge. Interestingly, an enzymatic activity that preferentially uses NRH as a substrate had been characterized previously. The enzyme NQO2, a quinoneoxidoreductase, is known to use NRH preferentially as the upstream reductant, in a reaction which converts quinones to dihydroquinones (25,26). However, the effects of NRH in altering cellular NAD$^+$ levels have remained unexamined in the published literature. In this manuscript we report properties of NRH as an enhancer of cellular NAD$^+$ concentrations. NRH is effective in this respect in mammalian cells and in mice tissues. NRH acts at equal or lower concentrations than those observed for NR and NMN and surpasses NR and NMN in biological effect *in vitro* and *in vivo*. We identify a putative biochemical mechanism of action wherein NRH represents a starting point for a novel biosynthetic pathway to NAD$^+$

RESULTS

Preparation of NRH In order to better investigate the properties of NRH (Scheme 1) as a potential NAD$^+$ precursor, a method of preparation of the compound was required, preferably by direct chemical synthesis. We prepared the compound from nicotinamide riboside triflate, via published synthetic methodology developed by our laboratory (17). NR(triflate) was reduced in aqueous solution in 50 mM potassium phosphate pH 8.6 with 0.80 equivalents of sodium dithionite, followed by immediate purification on C-18 resin to provide purified NRH (Scheme 1, See Experimental Procedures). The ^{1}H NMR spectrum agreed with a prior literature report for this compound (see Supporting Information for ^{1}H NMR and ^{13}C NMR spectra). Additional properties of NRH are provided in the Supporting Information, including its UV spectrum which is centered at 340 nm (See Figure S1). The compound is strongly fluorescent, (excitation wavelength = 340 nm), similar to NADH. NRH has moderate chemical stability at pH values below 7, with a half-life of decomposition of 3 hr at 37 °C at pH 6.0 (Figure S2). Consequently, only freshly prepared NRH solutions were used in all experiments.

NAD$^+$ Concentration Increases Caused by Exposure to NRH To assess if NRH can be absorbed by cells and change NAD$^+$ concentrations we exposed a number of mammalian cell lines, including insulinogenic (INS1, MIN6), neuron-like (F98, U87, LN229), muscle-like (C2C12), and HEK293 cells with vehicle, 1 mM NR or 1 mM NRH for time periods of 6 hr. Cellular NAD$^+$ concentrations were determined in accord with our published assay (27). Changes in NAD$^+$ concentrations were 2.4-10 fold for cells exposed to NRH, well above levels reported for any other NAD$^+$ precursor yet studied (Figure 1a). In each cell line, NRH exceeded the NAD$^+$ concentration enhancement caused by NR by at least 2 fold, and in all cases greatly exceeded the levels induced by NMN (See Figure S3). These data establish that NRH is effective in stimulating NAD$^+$ increases compound in cultured mammalian cells superior to NR or NMN. To further confirm the NAD$^+$ enhancement effect of NRH, we examined an additional neuron-derived cell line (Neuro2a) treated with NRH, which caused an approximately 10 fold increase in NAD$^+$ concentrations compared to control (Figure 1b), an enhancement for an NAD precursor which is unprecedented to our

knowledge. To unequivocally confirm increased NAD$^+$ production, lysate obtained from Neuro2a cells treated for 6 hr with NRH was analyzed using HPLC to directly detect the increased NAD$^+$ amount using an untreated control as a comparison and employing an NAD$^+$ standard to confirm identity. As shown in Figure 1c, NRH substantially increased the peak corresponding to NAD$^+$ by many-fold in the NRH treated lysate mixture, well above the level for control. To validate our other NAD$^+$ measurements, we checked for possible interference of NRH in the plate reader assay typically employed (27), but minimal interference from NRH was observed when the assay was performed at relevant NRH concentrations (See Supporting Information for detail). Thus, we can conclude by two independent assays (HPLC and plate reader NAD$^+$ assay) that NAD$^+$ concentrations are substantially increased by NRH exposure to cultured mammalian cells.

A dose-response profile for NRH on NAD$^+$ concentration was obtained in Neuro2a cells. Concentrations of NRH in media were varied from 100 μM to 2000 μM for a period of 6 hours. NAD$^+$ concentration increase reached greater than 10 fold (Figure 2a). Maximal NAD$^+$ increase was determined by theoretical fit of the curve

$$[NAD^+] = B_{max}[NRH]/([NRH] + EC_{50}) + B_0$$

where B_{max} is maximum biological effect caused by NRH, EC50 is concentration to achieve 50 percent of B_{max} and B_0 is the untreated control NAD$^+$ concentration. The values obtained were B_{max} = 11200 pmol/10^6 cells and EC50 was found to be 310 μM. The value for B_0 was 690 pmol/10^6 cells. According to the curve, the concentration of NRH required to achieve 260 percent NAD$^+$ concentration increase as compared to control was determined to be 34 μM, whereas 1 mM NR is required to achieve the same increase in this cell line (17), and NMN does not achieve doubling of NAD$^+$ concentration at 1 mM (Figure S3). These data provide a relative potency increase of approximately 30 fold versus NR for this cell line. A dose-response profile was also determined for primary neurons, obtained as previously described (28). These cells were treated with increasing concentrations of NRH for a period of 6 hr. At the lowest concentration of NRH tested, 100 μM, neuronal NAD$^+$ concentrations were approximately 5 fold elevated over corresponding controls, and saturation was reached at 500 μM, where concentrations reached 7.5 fold over untreated controls. To further investigate if NRH can alter sub-compartment NAD$^+$ concentrations, we measured mitochondrial NAD$^+$ content which is known to increase with some NAD$^+$ concentration enhancers, such as NR (14). This compartment had increased NAD$^+$ concentrations of at least 3.5 fold in Neuro2a cells treated with NRH at 1 mM after 18 hr (Figure 2c).

Time courses for NRH action were also performed. Thus, Neuro2a cells and HEK293 cells were treated with NRH for different incubation times then harvested and NAD$^+$ contents assayed. We determined that the NAD$^+$ concentration elevating effects were present as early as 1 hour in HEK293 cells, with full effects evident at 6 hr (Figure 2d). We saw a similar strong effect in Neuro2a cells at 6 hr (Figure 2e). Robust NAD$^+$ elevation caused by treatment of NRH remained evident after 18 hr in HEK293 cells (Figure 2d), in part due to persistence of the majority NRH in media past a time of 18 hr (Figure S2).

Lack of Toxicity and Rescue Effects in Genotoxicity These large increases in NAD$^+$ concentrations caused us to wonder about possible toxicity to cells. We did not observe any appreciable loss of cells in culture from exposure to 1 mM NRH for 24 hr (Figure S4). For example, cell counts were similar between controls and NRH treated cells for Neuro2a although cell counts were slightly lower in HEK293 cells after 24 hr. Trypan blue positive cells were similar in both cases, not exceeding 3 percent, and there were no significant differences in apoptotic markers. Annexin V or Caspase 3/7 in NR and NRH treated cells versus controls, indicating no changes in apoptotic pathway activation (Figure S4).

NRH is a reductant and we considered that it could potentially cause changes to NAD$^+$/NADH ratio. Thus, we measured the ratio after NRH treatment. NAD$^+$/NADH ratio is regulated in cells and is typically highly oxidizing under most

physiological conditions (29). However, the effect on this ratio upon increasing NAD$^+$ concentrations up to 10 fold from resting levels has not been assessed, to our knowledge. Thus, we treated cells for 6 hr with NRH and measured NAD$^+$ concentration and NADH concentration independently (27) to determine absolute amounts of NAD$^+$ and absolute amounts of NADH. We found that NAD$^+$ concentrations were substantially increased as expected, but NADH concentrations were not increased proportionally (Figure 2e). Thus, a consistent effect of NRH treatment is a net increase in the NAD$^+$/NADH ratio in 4 different mammalian cell lines (Figure 2f). Interestingly, Canto et al. reported (14) that NR-induced NAD$^+$ increase in animal tissues caused an increased NAD$^+$/NADH ratio. As another way to identify perturbation in NAD$^+$/NADH ratio, we measured lactate concentrations in cell culture. Both intracellular lactate levels and extracellular lactate were measured at times of 6 hr. We saw no statistically significant increases in lactate in media, and intracellular lactate levels were largely unaffected, except in one instance, where intracellular lactate was substantially depleted within HEK293 cells (Figure S5). The preceding results showed that mM concentrations of NRH are well tolerated by cells, and that highly elevated NAD$^+$ levels are well tolerated and do not lead to obvious toxic effects, at least over a 24 hr period.

Intrigued by the magnitude of NAD$^+$ concentration enhancement we wondered if NRH could improve cell survival under stressful conditions that deplete NAD$^+$. Thus, we examined genotoxicity, which causes DNA damage and activates polyADPribosylpolymerases and causes NAD$^+$ depletion (30). Strong genotoxicity can lead cells to severely deplete NAD$^+$, leading to cell death (5). Thus, we treated Neuro2a cells with hydrogen peroxide (HP) for a period of 6 hr and then counted cells and measured NAD$^+$ in samples either co-treated with NRH (1 mM) or with vehicle. We found that cell survival improved from 10 percent (HP) to nearly 80 percent with HP + NRH treatment (Figure 3a). In addition, NAD$^+$ levels remained highly elevated in HP + NRH treated cells, whereas in HP cells NAD$^+$ concentrations became substantially depleted below control values (Figure 3). Similar results were obtained with INS1 cells, which are insulin containing cells and sensitive to HP. Cell survival went completely to zero in HP treatment but was increased to nearly 50 percent in HP + NRH (Figure 3b). We then compared NR effects with NRH in Neuro2a cells at a lower concentration of 250 µM, and found that NRH is still protective, of not only NAD$^+$ level, but in cell survival, whereas, although NR treatment is also effective, it does so much less well, in both preservation of NAD$^+$ content as well as cell viability (Figure 3c).

To broaden these findings, we examined the alkylative genotoxin methylmethane sulfonate (MMS), which we have used in past studies (5), on Neuro2a and HEK293 cells. Cell survival in Neuro2a cells improved with NRH co-treatment with MMS, with survival reaching near 100 percent, indicating full protection in MMS +NRH treated samples. NAD$^+$ concentrations plummeted in this case, to below untreated control value, but were still higher than MMS treatment alone (Figure 3d). In HEK293 cells, survival was improved considerably from 20 percent (MMS) to nearly 80 percent (MMS+NRH; Figure 3e). Furthermore, MMS + NRH treated cells had higher NAD$^+$ concentrations versus MMS treatment alone. Thus, challenge to cells with genotoxicity identifies conditions where NRH substantially improves cell survivability, concurrently protecting the cellular NAD$^+$ pool from depletion. Again, we compared NR with NRH at 250 µM (Figure 3f), and found that NR could not provide protection of cells at this concentration, and only modestly improved NAD$^+$ levels versus untreated controls, whereas NRH provided statistically significant increases in cell survival as well as increased NAD$^+$ concentrations versus corresponding MMS treated control.

The differences in NAD$^+$ concentrations observed at 6 hours in cells for the two genotoxins appear to arise from differing lifetimes of the genotoxins in cell culture. Peroxide is depleted rapidly in cell culture (See standard curve and depletions in Figure 3g and Figure 3h respectively). Rapid depletion of peroxide allows rebound to the NAD$^+$ concentrations in NRH treated cells at 6 hours. On the other hand, MMS persists in cell culture past 6 hours (See standard curve and depletions in Figure 3i and Figure 3j respectively). This stability explains persistent depletion of NAD$^+$

concentrations at harvest, even in NRH treated cells.

Possible Biochemical Mechanisms of NRH-Induced Increases to NAD$^+$

In order to better understand the possible mechanisms where NRH exposure to cells causes NAD$^+$ concentrations to accumulate, we sought to determine if NAD$^+$ turnover is inhibited by NRH treatment. Therefore, we treated cells with [carbonyl-^{14}C]nicotinamide (NAM) which becomes converted to [carbonyl-^{14}C]NAD$^+$ in cells as shown by HPLC (0 time, Figure 4a). After washing cells of residual radioactivity in media, we exposed labeled cells to NRH or vehicle and measured intracellular labeled NAD$^+$ as a function of time using HPLC and scintillation counting. Extracellular radioactivity in the form of released [carbonyl-^{14}C]NAM was also determined at each time point. Time dependent outcomes of the experiment (NRH versus control) are expected as follows: 1. No change in loss of label at each time for NRH treated samples is indicative of no inhibition of turnover by NRH. 2. Increased loss of label at each time for NRH samples is indicative of increased NAD$^+$ turnover and no inhibition of turnover by NRH and 3. Decreased label loss at each time for NRH samples is indicative of inhibition of NAD$^+$ turnover by NRH. Radiolabeled NAD$^+$ acts as a reporter for the entire NAD$^+$ pool, as there is no expected isotope effect on turnover for a carbonyl ^{14}C-label. Exposure of radiolabeled Neuro2a cells with 1 mM NRH resulted in rapid loss of label from NAD$^+$, with a half-life of less than 100 min (Figure 4a) whereas corresponding controls not exposed to NRH lose label to NAD$^+$ with an approximate half-life of 240 min (Figure 4a). Corresponding release of radioactivity to media is correlated to label loss (Figure 4a). Thus, exposure of cells to NRH accelerates radiolabel loss from intracellular NAD$^+$, which is consistent with increased NAD$^+$ reaction and degradation, i.e. NAD$^+$ consumption. This result provides evidence that NRH does not inhibit NAD$^+$ turnover. Thus, inhibition of NAD$^+$ consumption does not obviously contribute to NRH-induced NAD$^+$ concentration increase.

Increased NAD$^+$ consumption in the presence of NAD$^+$ accumulation in cells suggests that NRH causes a marked increase in NAD$^+$ biosynthesis. Since NRH provides a substantially higher accumulation effect than for other NAD$^+$ precursors, it suggests possible involvement of multiple biosynthetic pathways converging to NAD$^+$. One putative pathway is nicotinamide salvage. To investigate this pathway as a possible player in NRH effects, we treated cells with FK866 (31), a known inhibitor of the enzyme nicotinamide phosphoribosyltransferase (Nampt) which is responsible for NAM recycling to nicotinamide mononucleotide (NMN)(32). FK866 causes depletion of NAD$^+$ concentrations in both HEK293 (Figure 4b) and Neuro2a (Figure 4b) cells. Decline in NAD$^+$ is attributable to failure of released NAM to be resynthesized into NAD$^+$. Co-administration of NRH with FK866 completely rescues the effect of FK866 on cells. Moreover, FK866 has no effect on either NRH induced NAD$^+$ increases. Thus NRH induced NAD$^+$ concentration increases do not apparently require nicotinamide recycling for the effect. Similarly, NR increased NAD$^+$ concentrations and this effect was not very sensitive to FK866 (Figure 4b), consistent with the interpretation that NR utilizes a kinase dependent pathway independent of Nampt to provide the majority of its NAD$^+$ biosynthesis. Thus, NRH causes marked NAD$^+$ increases even when Nampt is inhibited, indicating a nicotinamide independent and Nampt independent mechanism of action.

Next, we asked if it is possible that cells possess an activity that can convert NRH to a subsequent product, which could be on the biosynthetic pathway to NAD$^+$. We thus treated Neuro2a cell lysates with ATP (2 mM) and NRH (100 μM) and monitored for formation of product. We found that in the absence of ATP no reaction of NRH was observed (data not shown), but in the presence of ATP a new product was formed, of identical retention time to the compound dihydronicotinamide mono-nucleotide (Figure 4c NMNH; prepared by degradation of NADH with snake venom diesterase). To our knowledge, this conversion of NRH to NMNH (Figure 4c, Neuro2a lysate at 37° C: specific activity = 0.38 ± 0.05 pmol/min/μg protein. See Figure 5 for structure of NMNH) has not previously been reported for cell lysates and provides a putative first metabolic step of NRH to NAD$^+$.

One possible mechanism for the conversion of NRH to NMNH could be action of known NR dependent kinases, Nrk1 and/or Nrk2. To ascertain whether NRH induction of NAD$^+$ accumulation in cells requires Nrk1, we obtained HAP1 wildtype and Nrk1 KO cell lines (See Experimental Procedures), and prepared protein lysates from these cell lines. With these lysates, we measured NR kinase activity by measurement of [^{14}C-carbonyl]NR conversion to [^{14}C-carbonyl]NMN in the presence of ATP. Conversion of NR to NMN in wildtype HAP1 lysate was easily measureable, but this activity was completely lost in corresponding Nrk1 KO lysate (Figure 4d). However, both wildtype and Nrk1 KO lysates retained NRH kinase activity, as shown by formation of NMNH in the presence of ATP (Figure 4e). The biological activity of Nrk1 is known to regulate NR conversion to NAD$^+$ in some cell lines. In HAP1 this also appears to be the case. HAP1 WT cells have statistically significant increase in NAD$^+$ concentrations when treated with NR, increasing to 190 % of untreated control, whereas the corresponding Nrk1 KO shows no effect for NR in increasing NAD$^+$ content (Figure 4f). Thus, Nrk1 is required for NR-induced NAD$^+$ increase in this cell line. On the other hand, WT and Nrk1 KO cell lines are both able to respond to NRH treatment, increasing 6.8 fold over untreated controls (Figure 4f). This result confirms that Nrk1 is not required for NRH conversion to NAD$^+$, consistent with results showing Nrk1 is also not required for conversion of NRH to NMNH (Figure 4e).

Finally, we investigated whether recombinant Nrk2 could phosphorylate NRH, and found that despite changes in pH from pH =7-9, recombinant Nrk2 could not measurably phosphorylate NRH (rate <0.005 s^{-1}) to the extent observed by Neuro2a lysate (Figure 4g). On the other hand, using [^{14}C-carbonyl]NR as a substrate, recombinant Nrk2 was clearly very active, exhibiting an observed rate of 3.07 s^{-1} under the same reaction conditions. Collectively, these experiments indicate that NRH is phosphorylated by a kinase not previously recognized to participate in NAD$^+$ metabolism to convert to it to NMNH. Moreover, NRH effects on NAD$^+$ concentrations appear to be independent of Nrk1 and Nrk2. These results lead us to propose that Path A (with elimination of Nrk1 or Nrk2 as possible kinases) depicted in Figure 5 likely accounts for the majority of biological action of NRH, and that Path B is not required for NRH effects on NAD$^+$ concentrations.

NRH in vivo Finally, in order to assess for biological effects in mice, we treated C57BL/6J mice by intraperitoneal injection with 1000 mg/kg NRH, and assessed NAD$^+$ contents in tissues at 4 hr. As can be observed in Figure 6, NAD$^+$ contents increased several fold in blood, brain, adipose, and kidney, with a greater than 5 fold increase in liver NAD$^+$ concentrations at 4 hr (Figure 5a). Weakest effects were observed in skeletal muscle, where increases were above control, but not statistically significant. Table 1 shows measured NAD$^+$ contents and observed errors. As shown by the data, NRH is an effective NAD$^+$ concentration enhancer in many animal tissues and organs upon single dose administration. To assess for possible perturbation of redox potential, we measured NADH content in liver, which is the most profoundly affected organ with NRH treatment. We determined a NAD/NADH ratio 68 ± 10 in NRH treated liver.

In order to determine if NRH is more effective than other NAD$^+$ precursors in vivo, we injected 250 mg/kg intraperitoneal doses of NRH or NMN or NR or vehicle only and measured NAD$^+$ contents in kidney and liver at 4 hr (Figure 5b). We found that in kidney NR, NRH and NMN statistically increased NAD$^+$ contents above control, with NRH providing the highest effect at 180 % with NR and NMN providing 159 and 156 % respectively. In liver, NRH increased NAD concentration by 540 %, while NR and NMN provided 132 % and 149 % respectively (Figure 5b). Thus, NRH provides larger NAD$^+$ increases than NR and NMN at equivalent doses, and in liver provides quite significant NAD$^+$ increase at a low dose, consistent with improved pharmacologic potency versus other NAD$^+$ precursors. These findings, recapitulate observations made with cell culture studies.

DISCUSSION

The discovery of novel agents to increase cellular NAD$^+$ is of recent high interest in the

biomedical research community with a number of ongoing clinical studies and several recent published ones involving the newly discovered NAD$^+$ enhancing agents NR and NMN (18, 19). In the current work the previously uninvestigated compound NRH was synthesized, and determined to be a potent and effective enhancer of NAD$^+$ concentrations in cultured cells as well as primary neurons. The maximal concentration enhancements were many fold over control values, and reached unprecedented levels of up to 10 fold in Neuro2a cells and over 7 fold in cultured primary neurons. These effects raise the bar for a pharmacological agent of this kind. NRH was found to exceed NR and NMN effects by several to many fold in this respect, suggesting a unique mechanism of action. Moreover in terms of potency, NRH achieved a 260% NAD$^+$ concentration versus control in Neuro2a cells at 34 μM, whereas NR required 1 mM for this same effect (17), indicating that NRH is approximately 30 times more potent than NR under these conditions. Similar doubling of NAD$^+$ concentrations occurred at NRH concentrations below 100 μM in primary neurons.

NRH has NAD$^+$ concentration enhancement effects requiring 1-6 hours to occur in cell culture and its effects can remain sustained for up to 18 hr. Effects reaching doubling of NAD$^+$ concentrations occurred in as fast as 1 hr (Figure 2d). Time courses for the effects of NAD$^+$ precursors on intracellular NAD$^+$ concentrations have remained largely unreported. Dose response profiles of NRH in both Neuro2a cells and primary neurons indicate EC50s (defined in Figure 2 legend) between 100-300 μM indicating a large dynamic concentration range for NRH action. Cell culture studies in at least 8 cell lines showed NRH was also able to substantially raise NAD$^+$ concentrations, and this activity of NRH was also observed in vivo. NRH injected by intraperitoneal administration increased NAD$^+$ concentrations many fold in a variety of mouse tissues (Table 1). The dose-response profile for NRH in mouse or any other animal remains to be established and is an objective of future research in the laboratory.

A concern with pharmacologic use of NAD$^+$ concentration enhancers is the prospect that they may cause an undesired cell toxicity or cause perturbations to NAD$^+$/NADH ratio. Cell counts were slightly decreased in HEK293 cells in 24 hr incubations as determined by cell counts, but there was no evidence for activation of apoptosis. Moreover, NAD$^+$/NADH ratio was markedly changed. NRH treatment after 6 hr caused marked increases in NAD$^+$ accumulation in cultured cells, but less pronounced increases to NADH concentrations. Consequently, the accumulation of NAD$^+$ shifts the NAD$^+$/NADH ratio higher, and suggests a strong homeostasis that keeps NADH concentrations relatively lower. At the highest dosage tested, NAD$^+$/NADH ratio in liver was increased to 68 ± 10 with NRH treatment. Prior reports in the literature for mouse liver NAD$^+$/NADH range from 1-10 (33) and in rat liver about 2-8 (29). However, in rat liver free NAD$^+$/NADH is in the range 10-700 depending on whether cytoplasm or mitochondria is measured (29). We speculate that the higher NAD$^+$/NADH ratio with NRH treatment likely is due to shifting the ratio toward the protein-unbound NAD$^+$/NADH ratio which is typically much higher than the protein-bound ratio (29). This effect could be a consequence of saturation of protein binding sites for NAD$^+$ and NADH in liver at higher NAD$^+$ concentrations, causing the overall ratio to move higher. The ramifications of consistent increase of NAD$^+$/NADH ratio in cells and tissues is an open question, although arguably it poises cells to become more oxidative and may increase metabolic capacity.

Increasing cellular NAD$^+$ pools by up to 10 fold suggests that NRH could compensate NAD$^+$ depletion caused by genotoxic stress. Cells treated with either peroxide or the alkylative genotoxin MMS were depleted of cellular NAD$^+$ and experienced cell death. In contrast, cells treated with toxin and NRH maintained higher NAD$^+$ concentrations and experienced increased cell survival. These studies provide proof of concept for NRH as a cellular NAD$^+$ protection agent and cell survival agent. Differences in cell responses to the two treatments appear to arise from lifetimes of MMS and HP in media in the presence of cells. MMS is persistent in media, and cells have depleted NAD$^+$ even after 6 hr treatment. HP treated cells experience rapid depletion of HP in media , leading to recovery in NAD$^+$ homeostasis at 6 hr.

Nevertheless, NRH is effective in protection of cell NAD$^+$ and cell viability in both genotoxic treatments and is more effective than NR in HEK293 in peroxide treatments (Figure 3c) and Neuro2a cells in MMS treatments (Figure 3f).

To our knowledge, previous research had not investigated NRH as an NAD$^+$ precursor, and prior work had only uncovered a substrate role for NRH in the action of NQO2 (34). The biogenic origin of NRH in cells and tissues is currently unknown, and its occurrence in mammalian cells is also undocumented. One possible downstream metabolic fate of NRH is conversion to NMNH, as demonstrated in cell lysates in this report. Studies to understand how NRH augments cellular NAD$^+$ concentrations revealed it is probably not inhibiting NAD$^+$ consumption. This was investigated by measurement of loss of [carbonyl-^{14}C]NAD$^+$ in Neuro2a cells treated with NRH or with vehicle. In fact, NRH treated cells had increased NAD$^+$ turnover, and this is likely because increased NAD$^+$ concentrations drive increased cellular demand for NAD$^+$. The specific origin of this increased demand for NAD$^+$ is unclear, but could be due to sub-saturation of enzymes that consume NAD$^+$ as a substrate. This idea has been postulated to account for the actions of NAD$^+$ precursors as drivers of cellular adaptation.

Consequently, the simplest explanation of NRH effects on NAD$^+$ concentration is that it acts as a biosynthetic precursor to NAD$^+$ via very efficient biosynthetic pathways. Figure 5 presents likely metabolic pathways emanating from extracellular NRH and converging upon NAD$^+$. Although it is possible NRH is converted outside of cells to another species, we consider it unlikely that oxidation to NR or further breakdown to nicotinamide is responsible for NRH action, since neither NR nor nicotinamide alone provide the NAD$^+$ concentration enhancement effects observed for NRH. Moreover, breakdown of NRH to nicotinamide in either extracellular or intracellular compartments is apparently not required for NRH effects. This can be inferred from lack of effect of FK866, a potent inhibitor of Nampt and nicotinamide recycling. It had no effect on NAD$^+$ concentration increases induced by NRH.

We hypothesize that NRH encountering cell membranes is internalized, via an unknown transporter, or transporters and is internalized intact as NRH (Figure 5). NRH is then be acted upon by a kinase which converts NRH to a putative species NMNH (Path A). We showed that cell lysates possess an ATP dependent activity capable of converting NRH to NMNH. The identity of this kinase is not Nrk1 as shown by use of HAP1 wildtype and HAP1 Nrk1 KO cells. KO cells lack the ability to phosphorylate NR, and to respond to NR in NAD$^+$ increase. However, HAP1 Nrk1 KO cells respond fully to NRH and respond equivalently to HAP1 wildtype cells. Moreover, we showed that recombinant Nrk2 cannot convert NRH to NMNH, although it can readily convert NR to NMN. The independence of NRH effects from Nrk1 activity implies that NRH is not acting as a precursor to NR (Path B, Figure 5) since Nrk1 regulates NR effects in HAP1 cells but is not required for NRH effects in this cell line. Moreover, there is virtually no remaining NR kinase activity in HAP1 Nrk1 KO cells as measured by activity assays (Figure 4d), implying poor to non-existent Nrk2 activity in this cell line. The current data indicates to us that an unidentified kinase is involved in the activity of NRH, acting most likely to form NMNH (Path A Figure 5) as demonstrated for HAP1 and Neuro2a lysates. The identification of this kinase and characterization of its role in NRH mediated NAD$^+$ biosynthesis is an objective of future work by our laboratory.

In summary, these findings reveal a powerful naturally occurring pharmacologic agent that can raise NAD$^+$ levels in mammalian cells and tissues, providing an exceptional new tool to investigate how changes in NAD$^+$ metabolism can alter cellular physiology.

EXPERIMENTAL PROCEDURES

Synthesis of dihydronicotinamide riboside "NRH" (1-((2R,3S,4R,5R)-3,4-dihydroxy-5-(hydroxymethyl)tetrahydrofuran-2-yl)-1,4-dihydropyridine-3-carboxamide). In a flame dried flask under an Argon atmosphere, Nicotinamide riboside (NR) (100mg, 0.24 mmol) was added to 10 ml of 50 m M potassium phosphate pH = 8.5 at 0 ^{o}C. After 5 minutes, 0.8 eq of sodium dithionate ($Na_2S_2O_4$) was added and then run reaction at 0 ^{o}C for 30 minutes. (Progress of the reaction was

monitored by HPLC: 70% of starting material was consumed after 30 minutes). The crude product was purified by C-18 column using water as eluent to obtain light yellow solid (**2**). Yield 70%.

Cell culture HEK293, Neuro2a, F98, U87, LN229 and C2C12 cells were cultured in Dulbecco's modified Eagle's medium (DMEM) supplemented with 10% fetal bovine serum, 100 U/ml penicillin and 100 µg/ml streptomycin. MIN6 cells were cultured in DMEM with 15% fetal bovine serum, 100 U/ml penicillin and 100 µg/ml streptomycin. INS1 cells were maintained in Roswell Park Memorial Institute (RPMI)-1640 with 11.1 mmol/l D-glucose supplemented with 10% fetal bovine serum, 100 U/ml penicillin and 100 µg/ml streptomycin, 10 mmol/l HEPES, 2 mmol/l L-glutamine, 1 mmol/l sodium pyruvate, and 50 µmol/l 2-mercaptoethanol. Primary neurons were harvested from the brains of neonatal rats and plated for overnight. Human nicotinamide riboside kinase (Nrk1) knockout HAP1 cell line and the corresponding wildtype HAP1 cells were purchased from Horizon Discovery, UK. HAP1 cells were cultured in Iscove's Modified Dulbecco's Medium (IMDM) with 10% fetal bovine serum, 100 U/ml penicillin and 100 µg/ml streptomycin. Cells were maintained in a humidified incubator supplied with 5% CO2/95% air at 37°C.

Identification of NRH and NAD$^+$ on HPLC Samples containing NRH or NAD$^+$ were injected into EC 250/4.6 Nucleosil 100-5 C18 column on a Hitachi Elite Lachrom HPLC system equipped with Diode Array Detector L-2450. The C18 column was eluted with 20 mM ammonium acetate at 1 mL/min for 25 min, then with 20 mM ammonium acetate and 20% methanol for 20 min. NRH was characterized by its peak at 340 nm, while NAD$^+$ was characterized by its peak at 260 nm.

Cellular NAD$^+$ measurement For NAD$^+$ measurements, cells were seeded in 6-well plates until they reached approximately 90% confluency. Cells were treated with the desired concentrations of NRH or NR or NMN from concentrated stocks dissolved in water. Cells were harvested with trypsin digestion after treatment time. Unless indicated, the NRH treatment duration was 6 hr. Cell numbers were counted using hemocytometer and trypan blue. The harvested cells were pelleted at 3000 × g for 3 min. After removing the remaining media, cells were lysed with 7% perchloric acid to preserve NAD$^+$, then neutralized with 2 M NaOH and 500 mM K_2HPO_4. The cellular NAD$^+$ levels were measured as previously published (27).

NADH measurement To measure intracellular NADH levels, cell pellets were harvested after NRH treatment as previously described and lysed in 0.1 M NaOH/1 mM EDTA then incubated at 80°C for 10 min to avoid NAD$^+$ contamination. The samples are then neutralized with 0.5 M HCl and 500 mM KH_2PO_4. The NADH levels were measured as published (27).

Mitochondrial isolation To measure the individual NAD$^+$ concentration in mitochondria, Neuro2a cells were seeded in a 10 cm^2 petri dish, then treated with 1 mM NRH for overnight. The cells were harvested with trypsin and pelleted by spinning at 3000x g for 5 min. The mitochondrial fractions were isolated using Mitochondrial Isolation Kit for Mammalian Cells (Thermo Scientific) according to manufacturer's manual. Protein concentrations were later measured using Bradford assay for normalization. NAD$^+$ concentrations were measured as reported (27).

Hydrogen peroxide stability test Hydrogen peroxide (HP) in growth media was measured by a plate reader assay (Sigma Aldrich Fluorimetric Hydrogen Peroxide Assay Kit MAK165). 100 µM HP was incubated with either HEK293 or Neuro2a cells, both at 80-90% confluency. Media was aliquoted at 0, 10, 20, 30, 40 and 60 min and assayed by dilution into 96 well plates according to manufacturers instructions. Curve fit of the points is to the equation [Peroxide]= A1 + A2*exp(-*k*t) where *k* is the observed rate constant, A1 is residual concentration of peroxide at infinite time and A2 is the starting peroxide concentration. A standard curve was generated with known peroxide concentrations to achieve quantitation for the biological samples.

Methyl methanesulfonate stability test Growth medium containing 1 mM methylmethane sulfonate (MMS) was incubated with 80% confluent HEK293 cells or Neuro2a cells in 6 well plates. At 0, 2 and 4 hr the concentration of MMS in media was determined by mixing 50 µL media with 5 µL 1 M nicotinamide. Samples were heated at 80 °C for 10 min. The reaction was subsequently diluted with 200 µL water, then injected onto a C-18 column on HPLC and eluted with 20 mM ammonium acetate followed by 20 mM ammonium acetate with 20% MeOH. N-methyl-nicotinamide (260 nm detection) eluted before unreacted nicotinamide and the peak area of N-methylnicotinamide was quantified. A standard curve with a range of MMS concentrations was obtained similarly in order to quantitate samples.

NAD$^+$ turnover To measure the NAD$^+$ turnover rate in presence or absence of NRH, Neuro2a cells were seeded into 6-well plate until ~90% confluent, and treated with 700,000 CPM of ^{14}C-NAM (Movarek Biochemicals) per well overnight. Cells were then washed with PBS twice and incubated with or without 1 mM NRH. Both media and cells were harvested at 0, 1.5, 3, 5 and 7 hr. Radioactivity of media was directly counted by scintillation counter (Beckman Coulter). Cells were trypinsized and pelleted, then extracted with 7% perchloric acid and injected onto HPLC. The NAD$^+$ peak was collected using the above mentioned elution system and counted for radioactivity.

FK866 effect on NAD$^+$ levels To understand effects of nicotinamide recycling on NRH action, Neuro2a and HEK293 cells were treated with vehicle or 20 nM FK866, an NAMPT inhibitor that blocks the synthesis of NMN from nicotinamide. Additional added components included vehicle, 1 mM NR or 1 mM NRH. Cells were harvested after 6 hr and NAD$^+$ measured as previously described (27).

Identification of NMNH on HPLC To measure NRH kinase activity, 100 µM NRH, 2 mM ATP and 5 mM Mg^{2+} were combined withNeuro2a protein lysate (122 µg protein) all prepared in 100 µL RIPA buffer (Amresco, Cat No. 653-100ml). Reactions were incubated for 30 min at 37 °C. Corresponding controls with no lysate or no ATP were also incubated. The reactions were then ceased by incubating at 60 °C for 2 min and then spun by microcentrifuge at maximum speed for 10 min at 4 °C to remove precipitated protein. Supernatant was injected onto a C-18 column on an HPLC system and eluted with 20 mM ammonium acetate. The conversion of NRH to NMNH was characterized by integration of peaks with detection wavelength of 340 nm. Authentic NMNH was prepared by digestion of NADH with snake venom diesterase. Authentic NMNH was used as a chromatographic standard.

Synthesis of ^{14}C-labeled NR To test NR phosphorylation activity of enzymes, [carbonyl-^{14}C]NR was prepared from [carbonyl-^{14}C]NAM (Moravek Biochemicals). First, 5 µCi radioactive NAM was added to 1 mM unlabeled NAM, 600 µM NAD$^+$ and 200 µM acetylated peptide JB12 (Rockefeller University Proteomics Resource Center) in the presence of 1 µM recombinant SirT1 protein in 100 µL of 20 mM KH_2PO_4 pH = 7. Reaction was incubated at 37°C for 1 hr and then quenched with 5 % TFA. The [carbonyl-^{14}C]NAD$^+$ product was purified by injection onto a C-18 column on HPLC eluted with 0.1% TFA at 1 mL/min for 25 min, then with 0.1% TFA and 20% MeOH for 20 min. The fraction containing [carbonyl-^{14}C]NAD$^+$ was dried by vacuum. [carbonyl-^{14}C]NAD$^+$ dissolved in 100 µL of 20 mM KH_2PO_4 pH = 7 and treated with snake venom diesterase and alkaline phosphatase at 37°C for 2 hr. The reaction was quenched by addition of 5 % TFA. The resulting [carbonyl-^{14}C]NR was purified by injection onto a C-18 column on HPLC and collected and dried, similar to the procedure described above. The concentration of [carbonyl-^{14}C]NR was determined by peak area and compared to an authentic weighed NR standard. Specific activity was determined by scintillation counting of a known amount of [carbonyl-^{14}C]NR.

HAP1 cell lysate activity test Human Nrk1 sequence was disrupted in HAP1 cell line by 1 bp insertion in exon 5 of transcript NM_017881 by Horizon Discovery, UK and the mutation was validated by sequencing result by the company.

Protein lysates from wildtype and human Nrk1 knockout HAP1 cells were extracted with RIPA buffer and quantified by Bradford assay. To test the lysate activity against NR, equal protein masses of wildtype and Nrk1 knockout HAP1 lysates were incubated with 100 µM NR containing 8,000 CPM [carbonyl-^{14}C]NR, 2 mM ATP, 5 mM Mg^{2+}, and 150 mM KH_2PO_4 at pH 7. After incubation at 37°C for 30 min, the reactions were quenched by adding 10% volume of 20% trifluoroacetic acid and incubated on ice for 5 min. [carbonyl-^{14}C]NMN and [carbonyl-^{14}C]NR were collected after injection onto a C-18 column on HPLC eluted with 20 mM ammonium acetate and 20% MeOH. Fractions containing NMN and NR were counted separately by scintillation counter. To test the lysate activity against NRH, equal mass of cell lysates were incubated with 2 mM NRH, 2 mM ATP, 5 mM Mg^{2+}, and 150 mM KH_2PO_4 at pH 9 at 37°C for 30 min. The protein in reaction was removed by passing the reaction mixture through a 10K Amicon Ultra centrifugal filter (Millipore). NMNH was identified at 340 nm using HPLC system mentioned above.

Human Nrk2 protein cloning and activity test Human Nrk2 sequence (NM_017881.2) was cloned into a pET28a plasmid and sequenced. The plasmid was transfected into BL21-Codon Plus cells (Cat #230280 Agilent Technologies) for protein expression. Induction of cultures at OD_{600}= 0.5 at 37 °C was followed by 4 hours continued growth, followed by centrifugation to pellet. Pellets were resuspended in 75 mM KH_2PO_4 pH = 7 (5 volumes) and lysozyme and DNase added to break cells and digest DNA. After 3 freeze-thaw cycles, lysates were clarified by centrifugation and added to Ni-agarose. His-tagged Nrk2 protein was eluted with 250 mM of imidazole, 75 mM KH_2PO_4, 200 mM NaCl pH 7.0. Bradford assay and silver staining were used to quantify the protein concentration and to visualize the purity of protein. Protein was combined with 15% glycerol, 1 mM DTT and frozen in aliquots at -80 °C until use. To determine protein activity, 100 nM Nrk2 protein was incubated with 500 µM NR, 5 mM Mg^{2+}, 2 mM ATP including 8,000 CPM [carbonyl-^{14}C]NR in the presence of 150 mM KH_2PO_4 at pH7, 37°C for 1 hr. NMN and NR were separated by HPLC and counted by scintillation counter for ^{14}C activity. For activity with NRH, assays were performed as above, except that pH was varied from 7-9. No NR was added, and 1 mM NRH was used, and reactions were monitored by HPLC as described previously.

NRH effects on NAD$^+$ in vivo Eight male C57BL/6J mice at 8 weeks old were purchased from Charles River and were housed in a polycarbonate cage under a 12-hour-light/-dark cycle with free access to food and water. Then the mice were randomly assigned to three groups and received an intraperitoneal injection of either 1000 mg/kg NRH dissolved in PBS, or only PBS in control group. After 4 hours, these mice were subjected to cardiac puncture for blood collection and sacrificed. Blood was collected into tubes containing EDTA (BD Vacutainer) and centrifuged for 20 min at 5000 × *g* at 4°C and then plasma was collected and stored at −80°C. Liver, kidney, brain, muscle, and epididymal adipose tissue were harvested, immediately frozen in liquid nitrogen, then stored at -80ºC until NAD$^+$ analyses. To understand the effect of NRH in comparison with NMN and NR at a lower dosage, a similar experiment was done with intraperitoneal injection of one of the following 250 mg/kg NRH, 250 mg/kg NR or 250 mg/kg NMN or PBS and the mice were sacrificed after 4 hr for tissue collection. All procedures were approved by the Institutional Animal Care and Use Committee of Weill Cornell Medicine. For NAD$^+$ analysis, ~100 mg frozen tissue was pulverized in liquid nitrogen and homogenized in 7% perchloric acid by sonication, then the solution was neutralized and subjected to NAD$^+$ measurement as described above. For NADH measurement, ~100 mg frozen tissue was pulverized in liquid nitrogen and homogenized in water by sonication, then heated at 80 ºC for 2 min. The extractions were then centrifuged and injected onto HPLC. NADH peak was quantified at 340 nm and the concentration determined by an NADH standard.

Acknowledgments: This work was funded in part by NIH grant GM R01-106072 (AAS) and from NY Spinal Cord Research Board Contract C32098GG (AAS).

Conflict of interest: The authors Anthony A Sauve, Yue Yang and Farheen Sultana Mohammed have filed a patent on aspects of this work in conjunction with Cornell University. Anthony A Sauve has intellectual property related to NR and derivatives of NR. Chromadex Inc of Irvine California has a license on intellectual property related to production and uses of NR. Anthony A Sauve is a consultant and a co-founder of Metro MidAtlantic Biotech LLC and Metro International Biotech LLC.

REFERENCES

1. Yang, Y., and Sauve, A. A. (2016) NAD+ metabolism: Bioenergetics, signaling and manipulation for therapy. *Biochimica et biophysica acta* **1864**, 1787-1800
2. Belenky, P., Bogan, K. L., and Brenner, C. (2007) NAD+ metabolism in health and disease. *Trends in biochemical sciences* **32**, 12-19
3. Canto, C., Menzies, K. J., and Auwerx, J. (2015) NAD(+) Metabolism and the Control of Energy Homeostasis: A Balancing Act between Mitochondria and the Nucleus. *Cell metabolism* **22**, 31-53
4. Hassa, P. O., Haenni, S. S., Elser, M., and Hottiger, M. O. (2006) Nuclear ADP-ribosylation reactions in mammalian cells: where are we today and where are we going? *Microbiology and molecular biology reviews : MMBR* **70**, 789-829
5. Yang, H., Yang, T., Baur, J. A., Perez, E., Matsui, T., Carmona, J. J., Lamming, D. W., Souza-Pinto, N. C., Bohr, V. A., Rosenzweig, A., de Cabo, R., Sauve, A. A., and Sinclair, D. A. (2007) Nutrient-sensitive mitochondrial NAD+ levels dictate cell survival. *Cell* **130**, 1095-1107
6. Katsyuba, E., and Auwerx, J. (2017) Modulating NAD(+) metabolism, from bench to bedside. *The EMBO journal* **36**, 2670-2683
7. Sauve, A. A. (2008) NAD+ and vitamin B3: from metabolism to therapies. *The Journal of pharmacology and experimental therapeutics* **324**, 883-893
8. Scheibye-Knudsen, M., Mitchell, S. J., Fang, E. F., Iyama, T., Ward, T., Wang, J., Dunn, C. A., Singh, N., Veith, S., Hasan-Olive, M. M., Mangerich, A., Wilson, M. A., Mattson, M. P., Bergersen, L. H., Cogger, V. C., Warren, A., Le Couteur, D. G., Moaddel, R., Wilson, D. M., 3rd, Croteau, D. L., de Cabo, R., and Bohr, V. A. (2014) A high-fat diet and NAD(+) activate Sirt1 to rescue premature aging in cockayne syndrome. *Cell metabolism* **20**, 840-855
9. Zhu, X. H., Lu, M., Lee, B. Y., Ugurbil, K., and Chen, W. (2015) In vivo NAD assay reveals the intracellular NAD contents and redox state in healthy human brain and their age dependences. *Proceedings of the National Academy of Sciences of the United States of America* **112**, 2876-2881
10. Verdin, E. (2015) NAD(+) in aging, metabolism, and neurodegeneration. *Science* **350**, 1208-1213
11. Mouchiroud, L., Houtkooper, R. H., and Auwerx, J. (2013) NAD(+) metabolism: a therapeutic target for age-related metabolic disease. *Critical reviews in biochemistry and molecular biology* **48**, 397-408
12. Ryu, D., Zhang, H., Ropelle, E. R., Sorrentino, V., Mazala, D. A., Mouchiroud, L., Marshall, P. L., Campbell, M. D., Ali, A. S., Knowels, G. M., Bellemin, S., Iyer, S. R., Wang, X., Gariani, K., Sauve, A. A., Canto, C., Conley, K. E., Walter, L., Lovering, R. M., Chin, E. R., Jasmin, B. J., Marcinek, D. J., Menzies, K. J., and Auwerx, J. (2016) NAD+ repletion improves muscle function in muscular dystrophy and counters global PARylation. *Science translational medicine* **8**, 361ra139
13. Gariani, K., Menzies, K. J., Ryu, D., Wegner, C. J., Wang, X., Ropelle, E. R., Moullan, N., Zhang, H., Perino, A., Lemos, V., Kim, B., Park, Y. K., Piersigilli, A., Pham, T. X., Yang,

Y., Ku, C. S., Koo, S. I., Fomitchova, A., Canto, C., Schoonjans, K., Sauve, A. A., Lee, J. Y., and Auwerx, J. (2016) Eliciting the mitochondrial unfolded protein response by nicotinamide adenine dinucleotide repletion reverses fatty liver disease in mice. *Hepatology* **63**, 1190-1204

14. Canto, C., Houtkooper, R. H., Pirinen, E., Youn, D. Y., Oosterveer, M. H., Cen, Y., Fernandez-Marcos, P. J., Yamamoto, H., Andreux, P. A., Cettour-Rose, P., Gademann, K., Rinsch, C., Schoonjans, K., Sauve, A. A., and Auwerx, J. (2012) The NAD(+) precursor nicotinamide riboside enhances oxidative metabolism and protects against high-fat diet-induced obesity. *Cell metabolism* **15**, 838-847
15. Langley, B., and Sauve, A. (2013) Sirtuin deacetylases as therapeutic targets in the nervous system. *Neurotherapeutics : the journal of the American Society for Experimental NeuroTherapeutics* **10**, 605-620
16. Qin, W., Yang, T., Ho, L., Zhao, Z., Wang, J., Chen, L., Zhao, W., Thiyagarajan, M., MacGrogan, D., Rodgers, J. T., Puigserver, P., Sadoshima, J., Deng, H., Pedrini, S., Gandy, S., Sauve, A. A., and Pasinetti, G. M. (2006) Neuronal SIRT1 activation as a novel mechanism underlying the prevention of Alzheimer disease amyloid neuropathology by calorie restriction. *The Journal of biological chemistry* **281**, 21745-21754
17. Yang, T., Chan, N. Y., and Sauve, A. A. (2007) Syntheses of nicotinamide riboside and derivatives: effective agents for increasing nicotinamide adenine dinucleotide concentrations in mammalian cells. *Journal of medicinal chemistry* **50**, 6458-6461
18. Yoshino, J., Baur, J. A., and Imai, S. I. (2018) NAD(+) Intermediates: The Biology and Therapeutic Potential of NMN and NR. *Cell metabolism* **27**, 513-528
19. Rajman, L., Chwalek, K., and Sinclair, D. A. (2018) Therapeutic Potential of NAD-Boosting Molecules: The In Vivo Evidence. *Cell metabolism* **27**, 529-547
20. Martens, C. R., Denman, B. A., Mazzo, M. R., Armstrong, M. L., Reisdorph, N., McQueen, M. B., Chonchol, M., and Seals, D. R. (2018) Chronic nicotinamide riboside supplementation is well-tolerated and elevates NAD(+) in healthy middle-aged and older adults. *Nature communications* **9**, 1286
21. Dellinger, R. W., Santos, S. R., Morris, M., Evans, M., Alminana, D., Guarente, L., and Marcotulli, E. (2017) Repeat dose NRPT (nicotinamide riboside and pterostilbene) increases NAD(+) levels in humans safely and sustainably: a randomized, double-blind, placebo-controlled study. *NPJ aging and mechanisms of disease* **3**, 17
22. Trammell, S. A., Schmidt, M. S., Weidemann, B. J., Redpath, P., Jaksch, F., Dellinger, R. W., Li, Z., Abel, E. D., Migaud, M. E., and Brenner, C. (2016) Nicotinamide riboside is uniquely and orally bioavailable in mice and humans. *Nature communications* **7**, 12948
23. Gomes, A. P., Price, N. L., Ling, A. J., Moslehi, J. J., Montgomery, M. K., Rajman, L., White, J. P., Teodoro, J. S., Wrann, C. D., Hubbard, B. P., Mercken, E. M., Palmeira, C. M., de Cabo, R., Rolo, A. P., Turner, N., Bell, E. L., and Sinclair, D. A. (2013) Declining NAD(+) induces a pseudohypoxic state disrupting nuclear-mitochondrial communication during aging. *Cell* **155**, 1624-1638
24. Gong, B., Pan, Y., Vempati, P., Zhao, W., Knable, L., Ho, L., Wang, J., Sastre, M., Ono, K., Sauve, A. A., and Pasinetti, G. M. (2013) Nicotinamide riboside restores cognition through an upregulation of proliferator-activated receptor-gamma coactivator 1alpha

regulated beta-secretase 1 degradation and mitochondrial gene expression in Alzheimer's mouse models. *Neurobiology of aging* **34**, 1581-1588

25. Riches, Z., Liu, Y., Berman, J. M., Walia, G., and Collier, A. C. (2017) The ontogeny and population variability of human hepatic dihydronicotinamide riboside:quinone oxidoreductase (NQO2). *Journal of biochemical and molecular toxicology*
26. Megarity, C. F., Gill, J. R., Caraher, M. C., Stratford, I. J., Nolan, K. A., and Timson, D. J. (2014) The two common polymorphic forms of human NRH-quinone oxidoreductase 2 (NQO2) have different biochemical properties. *FEBS letters* **588**, 1666-1672
27. Li, W., and Sauve, A. A. (2015) NAD(+) content and its role in mitochondria. *Methods in molecular biology* **1241**, 39-48
28. Brochier, C., Jones, J. I., Willis, D. E., and Langley, B. (2015) Poly(ADP-ribose) polymerase 1 is a novel target to promote axonal regeneration. *Proceedings of the National Academy of Sciences of the United States of America* **112**, 15220-15225
29. Williamson, D. H., Lund, P., and Krebs, H. A. (1967) The redox state of free nicotinamide-adenine dinucleotide in the cytoplasm and mitochondria of rat liver. *The Biochemical journal* **103**, 514-527
30. Yang, T., and Sauve, A. A. (2006) NAD metabolism and sirtuins: metabolic regulation of protein deacetylation in stress and toxicity. *The AAPS journal* **8**, E632-643
31. Hasmann, M., and Schemainda, I. (2003) FK866, a highly specific noncompetitive inhibitor of nicotinamide phosphoribosyltransferase, represents a novel mechanism for induction of tumor cell apoptosis. *Cancer research* **63**, 7436-7442
32. Wang, T., Zhang, X., Bheda, P., Revollo, J. R., Imai, S., and Wolberger, C. (2006) Structure of Nampt/PBEF/visfatin, a mammalian NAD+ biosynthetic enzyme. *Nature structural & molecular biology* **13**, 661-662
33. Hayashida, S., Arimoto, A., Kuramoto, Y., Kozako, T., Honda, S., Shimeno, H., and Soeda, S. (2010) Fasting promotes the expression of SIRT1, an NAD+ -dependent protein deacetylase, via activation of PPARalpha in mice. *Molecular and cellular biochemistry* **339**, 285-292
34. Wu, K., Knox, R., Sun, X. Z., Joseph, P., Jaiswal, A. K., Zhang, D., Deng, P. S., and Chen, S. (1997) Catalytic properties of NAD(P)H:quinone oxidoreductase-2 (NQO2), a dihydronicotinamide riboside dependent oxidoreductase. *Archives of biochemistry and biophysics* **347**, 221-228

ABBREVIATIONS AND FOOTNOTES

NAD+, nicotinamide adenine dinucleotide; NR, nicotinamide riboside; NRH, dihydronicotinamide riboside; NMNH, dihydronicotinamide mononucleotide .

Table 1. Tissue NAD$^+$ values in Ctrl and NRH treated C57/B6 mice

	NAD$^+$ concentration (pmol/mg weight)	
Tissue	**Ctrl**	**NRH**
Blood	23.9 ± 2.2	57.0 ± 4.6
Liver	834.9 ± 130.7	4488.1 ± 142.0
Kidney	590.8 ± 83.9	1833.1 ± 148.9
Brain	51.0 ± 13.5	112.9 ± 17.3
Muscle	274.3 ± 11.6	338.3 ± 91.9
Adipose	15.2 ± 5.9	41.3 ± 2.7

Data are presented as mean ± SEM.

FIGURE AND SCHEME LEGENDS

Scheme 1. Synthesis of dihydronicotinamide riboside (NRH) from nicotinamide riboside triflate.

Figure 1. NAD$^+$ increases in different mammalian cell lines. (a) F98, U87, LN229, HEK293, INS1, MIN6 and C2C12 cells were treated with either 1 mM NRH or 1 mM NR for 6 hr. Their cellular NAD$^+$ changes are expressed as fold over control. Data are expressed as mean ± SEM, n=6. (b) NRH induces NAD$^+$ increase in Neuro2a cells. The cellular NAD$^+$ content of Neuro2a cells treated with either 1 mM NRH or 1 mM NR for 6 hr. Data are expressed as mean ± SEM, n=4. **** indicates $p<0.0001$. (c) NAD$^+$ peaks in HPLC chromatograms of control Neuro2a cell lysates or cell lysates treated with 1 mM NRH or 1 mM NR. The absorbance is shown at 260 nm. Upper right panel shows representative spectrum of NAD$^+$ peak.

Figure 2. Effects of NRH in different scenarios (a) Dose-response of NRH in Neuro2a cells. Neuro2a cells were incubated with 100, 200, 500, 1000 and 2000 µM for 6 hour. Fit is described in text. (b) Dose-response of NRH in primary neurons extracted from neonatal rat brains. Primary neuron cells were incubated with 100, 250, 500, 750 and 1000 µM NRH for 6 hour. (c) Mitochondrial NAD$^+$ contents in Neuro2a cells treated with 1 mM NRH for 18 hr. Data are expressed as mean ± SEM, n=4. (d) NRH increased NAD$^+$ levels in a time dependent manner in HEK293 and Neuro2a cells. HEK293 cells were incubated with 1 mM NRH for 1, 3, 6 and 18 hr. Neuro2a cells were incubated with 1 mM NRH for 1 and 6 hr. Data are expressed as mean ± SEM, n=4. (e) NAD$^+$ and NADH values were measured side by side in Neuro2a, HEK293, INS1 and C2C12 cells treated with 1 mM NRH for 6 hr. (f) shows NAD$^+$/NADH ratios. Data are shown as mean ± SEM, n=4. *, $p<0.05$; **, $p<0.01$, ***, $p<0.001$, ****, $p<0.0001$.

Figure 3. NRH protects cells from genotoxicity. (a) Neuro2a cells and (b) INS1 cells were exposed to 500 µM hydrogen peroxide (HP) with or without the co-incubation of 1 mM NRH for 6 hr. (c) Neuro2a were treated with 500 µM HP in the presence either 250 µM NR or NRH for 6 hr. d) Neuro2a cells and (e) HEK293 cells were treated with 400 µM methylmethane sulfonate (MMS) with or without the co-incubation of 1 mM NRH for 6 hr. (f) HEK293 cells were treated with 400 µM MMS, with or without 250 µM NR or NRH. Their survival rate and cellular NAD$^+$ content are expressed as mean ± SEM, n=4. Different letter indicates significant difference

($p<0.05$) between groups. (g) Standard curve constructed with different concentrations of hydrogen peroxide (HP). (h) stability of 100 μM HP in media with cultured cells. Solid curve is for HEK293 cells, and dashed curve is for Neuro2a cells. Fit provided k values of 0.094 min^{-1} for Neuro2a cells and 0.160 min^{-1} for HEK293 cells. Maximal rate under the assay conditions was determined to be 9.4 μM min^{-1} at 100 μM for Neuro2a cells, and 16 mM min^{-1} for HEK293 cells corresponding to half-life of 7.25 min for Neuro2a cells and 4.33 min for HEK293 cells. (i) HPLC assay to quantify MMS concentration and resulting standard curve. (j) The amount of MMS left in media quantified with initial 1 mM MMS combined with HEK293 and Neuro2a cells at 0, 2 and 4 hr.

Figure 4. NRH conversion to NAD$^+$ via a kinase mechanism. a) NAD$^+$ turnover in Neuro2a cells treated with or without NRH. Neuro2a cells were incubated with [carbonyl-^{14}C]nicotinamide overnight then treated with or without 1 mM NRH. Radioactivity was counted in both media and NAD$^+$ purified and counted at 0, 90, 180, 300 and 420 min after the treatment. b) FK866 did not inhibit the NAD$^+$ raising effect of NRH. HEK293 and Neuro2a cells were treated with the Nampt inhibitor FK866 or vehicle with or without 1 mM NR or NRH for 6 hr. Data are expressed as mean ± SEM, n=4. Different letter indicates significant difference ($p<0.05$) between groups. c) NRH is converted to NMNH by cell lysate. After incubation with Neuro2a protein lysate for 30 min at 37 ^{o}C, a new peak, detected at 340 nm wavelength on HPLC chromatography, is identified as NMNH. Conditions are described in Experimental Procedures. Inset shows UV spectrum for this product. d) Protein lysate from wildtype HAP1 cells can convert [carbonyl-^{14}C]NR into [carbonyl-^{14}C]NMN, but the activity has been abolished in lysate from human Nrk1 knockout HAP1 cells. e) When using NRH as substrate, both lysates from wildtype and human Nrk1 knockout HAP1 cells generate NMNH. f) Wildtype and human Nrk1 knockout HAP1 cells were treated with either 1 mM NR or NRH for 6 hr and measured for NAD$^+$ content. Data are expressed as mean ± SEM, n=4. Different letter indicates significant difference ($p<0.05$) between groups. g) Neuro2a protein lysate produced NMNH from NRH in the presence of ATP. When using recombinant human Nrk2 protein in the reaction carried out in pH 7, 8 and 9 buffers, no significant NMNH peak can be

observed at 340 nm. The activity of recombinant human Nrk2 was validated using [carbonyl-^{14}C]NR as substrate, and compared to NRH activity quantified in the inset.

Figure 5. Illustration of putative pathways from extracellular NRH to NAD$^+$. NRH may be internalized via an unknown transporter as intact molecule, then is either directly phosphorylated (Path A) or oxidized to NR (Path B). Phosphorylation of NRH generates putative species NMNH (Path A), a putative intermediate, which would then be oxidized to NMN or further metabolized by nicotinamide mononucleotide adenylyltransferase 1 (Nmnat1), Nmnat2 or Nmnat 3 to produce NADH, then converge on NAD$^+$.

Figure 6. NRH increased tissue NAD$^+$ content in vivo. (a) After intraperitoneal injection of 1000 mg/kg NRH in male C57BL/6J mice for 4 hours, NAD$^+$ content in blood, liver, kidney, brain and epididymal adipose tissue were increased compared to control group. Data are shown as mean ± SEM, n=4, *, $p<0.05$; **, $p<0.01$; ***, $p<0.001$; ****, $p<0.0001$ when compared with control. (b) Male C57BL/6J mice were intraperitoneal injected with one of 250 mg/kg NRH, 250 mg/kg NMN, 250 mg/kg NR or vehicle and then sacrificed at 4 hours. Liver and kidney NAD$^+$ content were compared across groups. Data are presented as mean ± SEM, n=4. Different letter indicates significant difference ($p<0.05$) between groups.

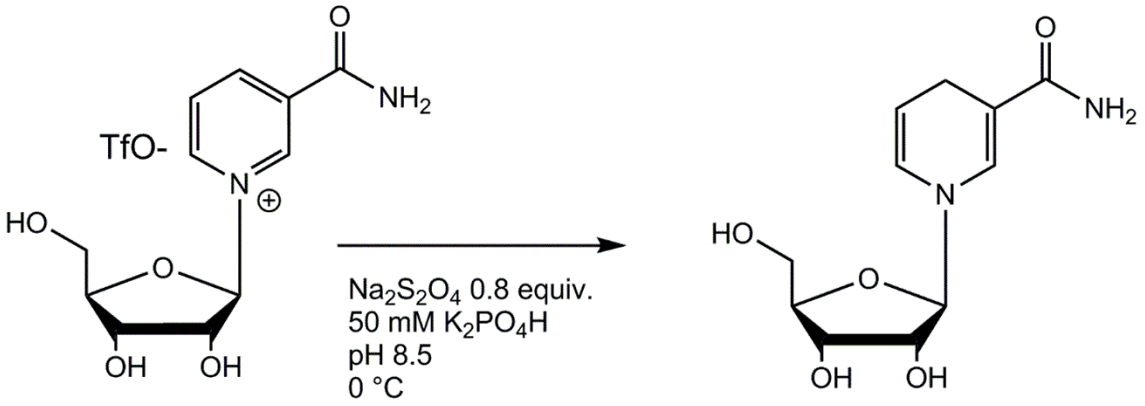

Nicotinamide riboside triflate

Dihydronicotinamide riboside "NRH"

Yang et al. Scheme 1.

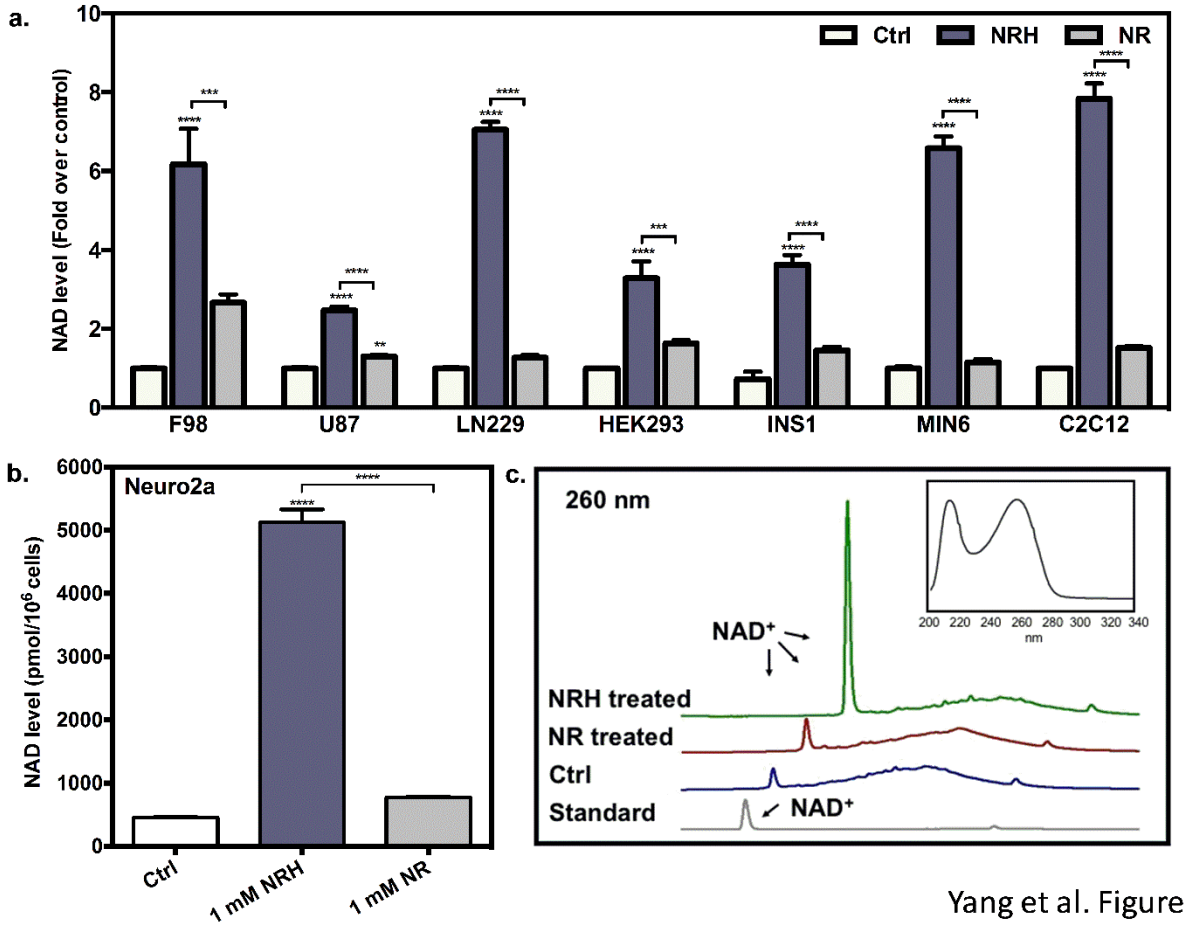

Yang et al. Figure 1

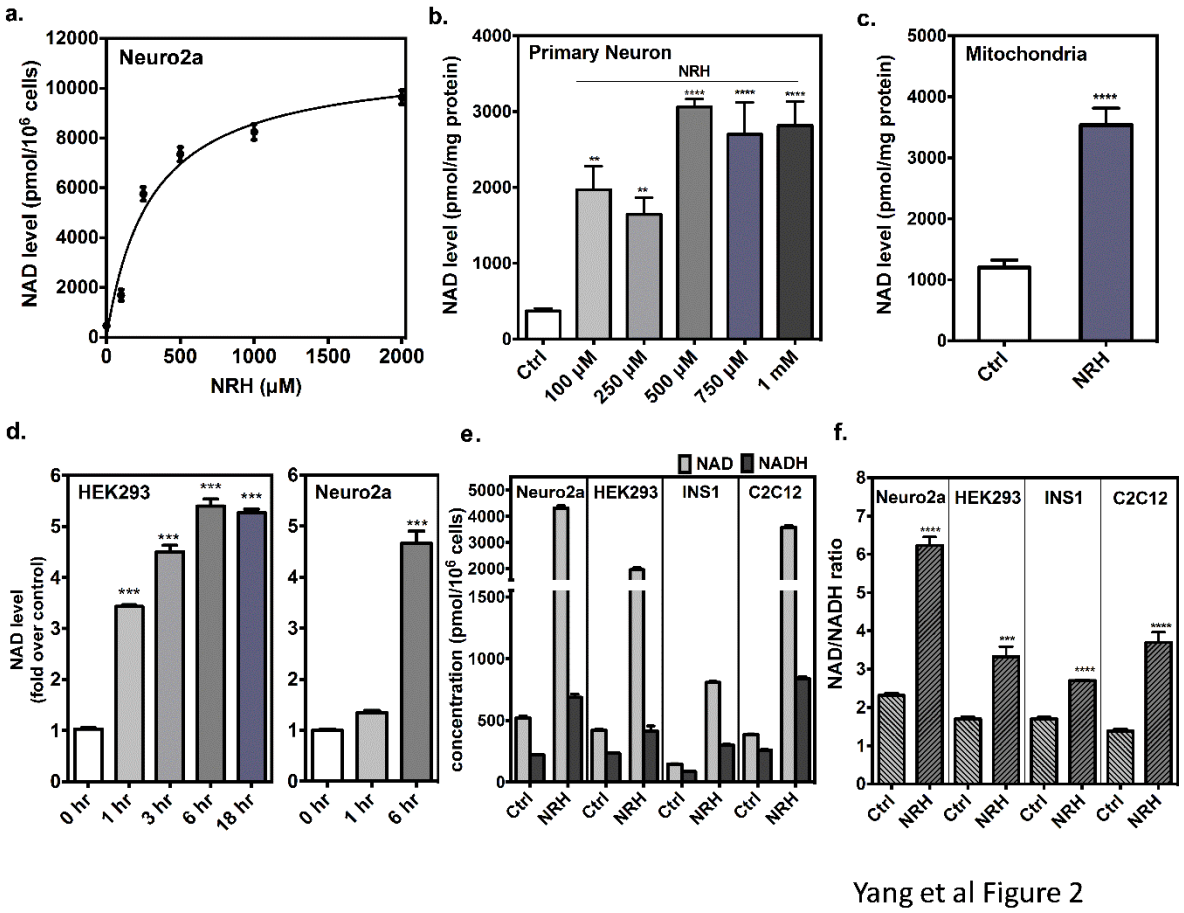

Yang et al Figure 2

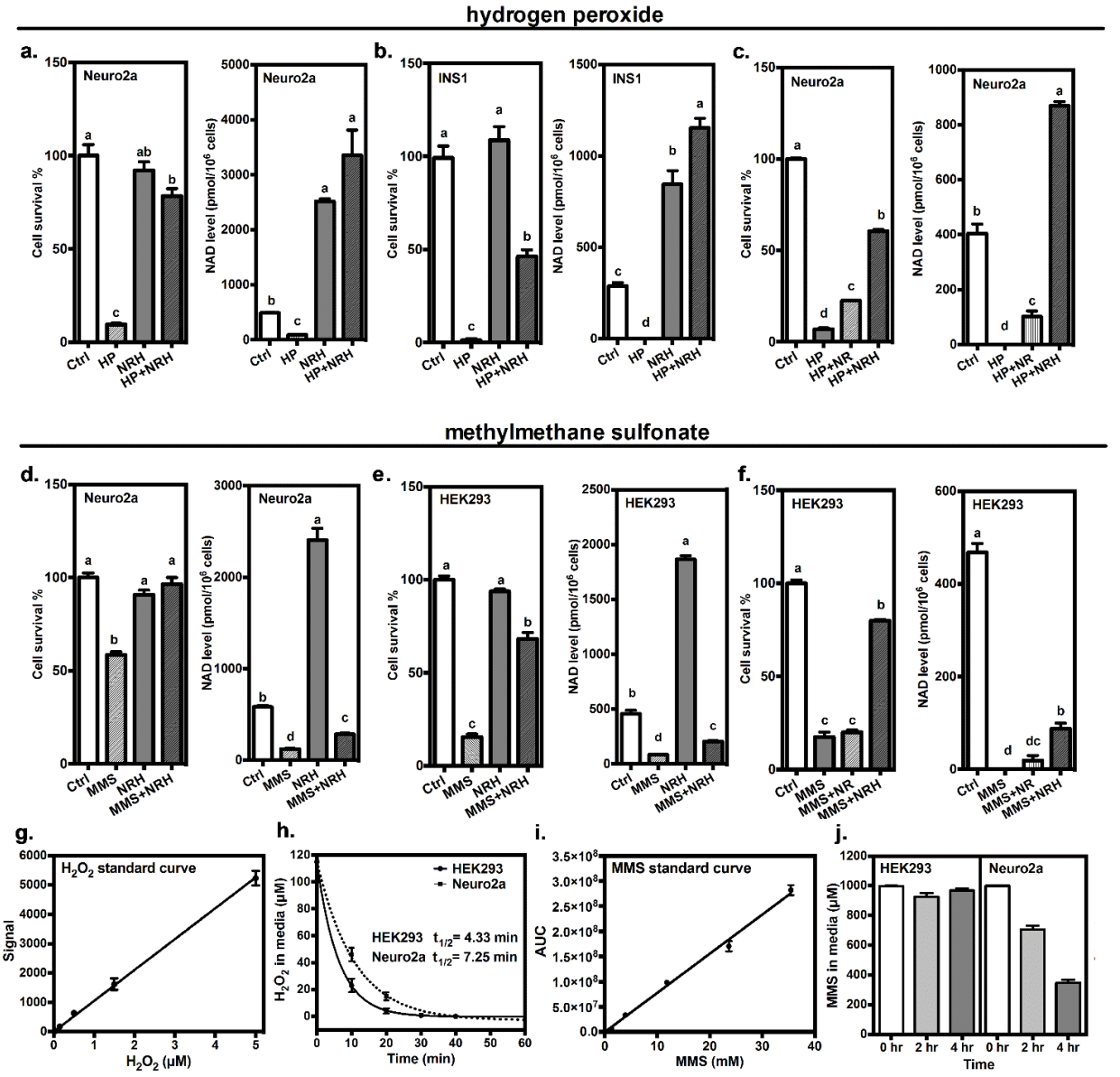

Yang et al Figure 3

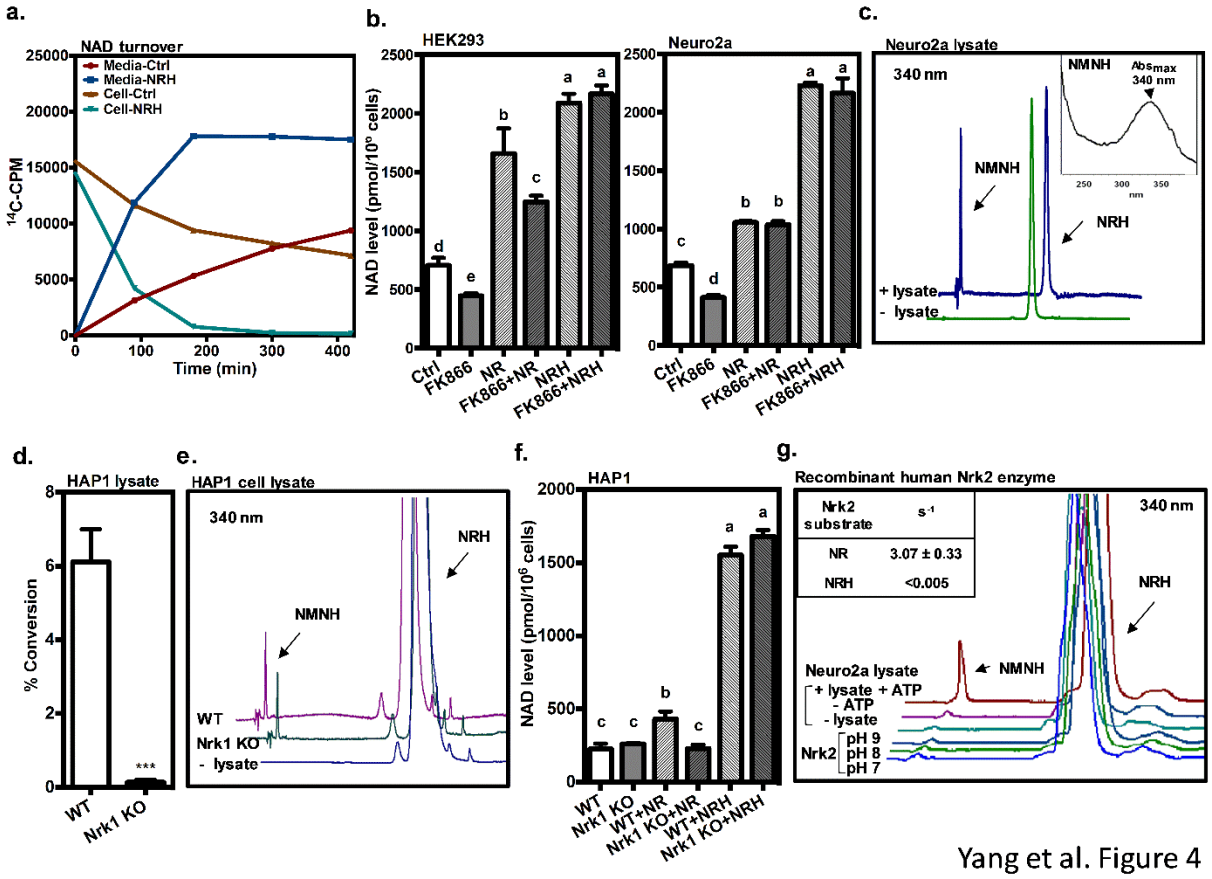

Yang et al. Figure 4

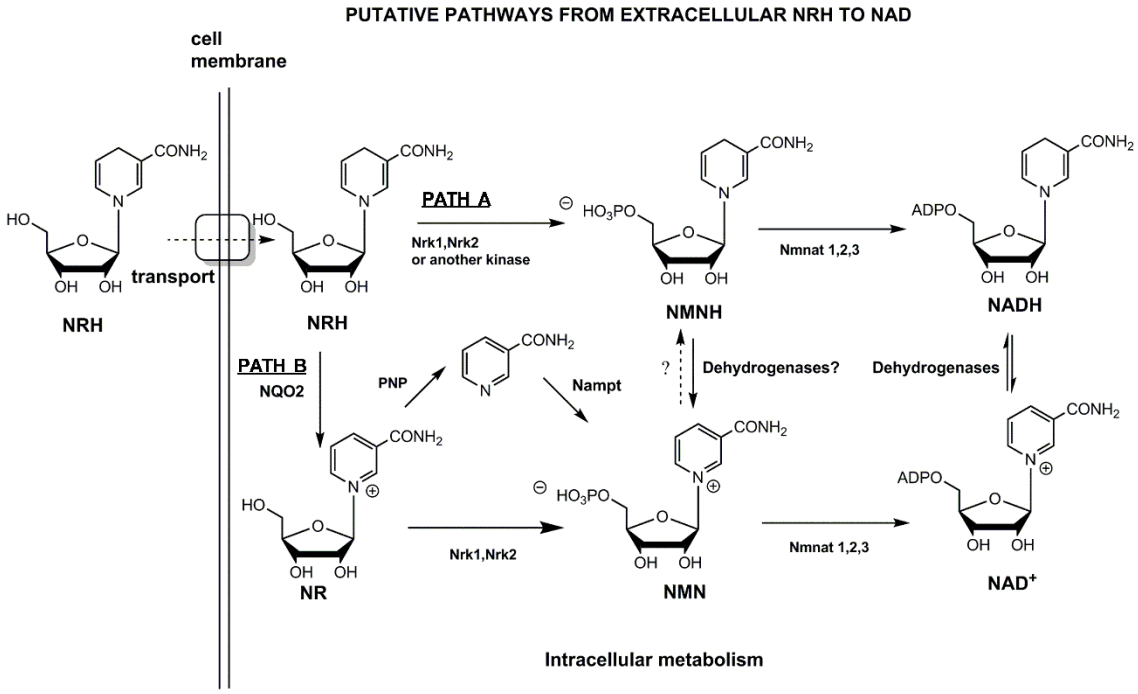

Yang et al. Figure 5

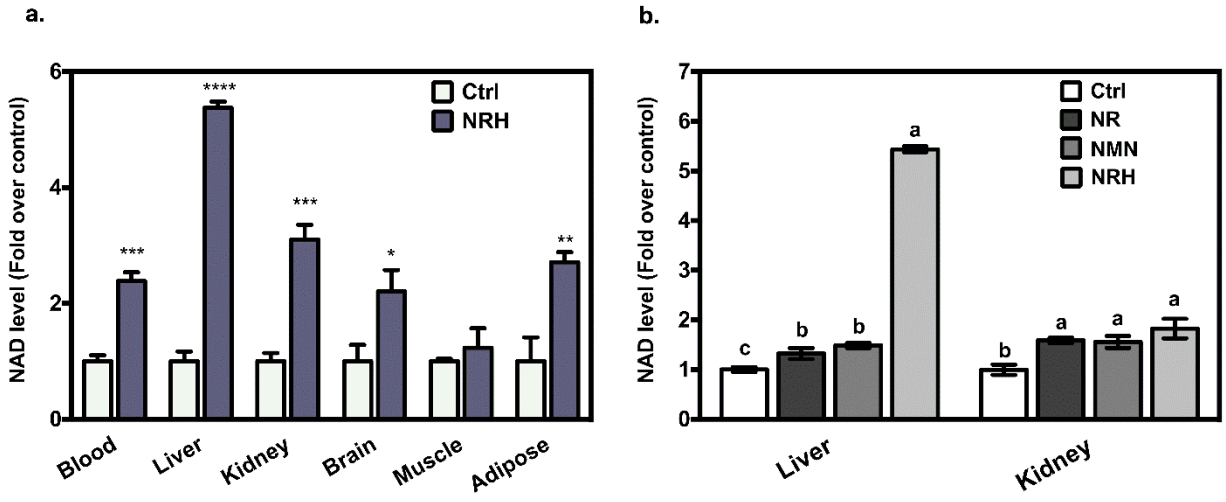

Yang et al. Figure 6

Dihydronicotinamide riboside is a potent NAD^+ concentration enhancer in vitro and in vivo

Yue Yang, Farheen Sultana Mohammed, Ning Zhang and Anthony A. Sauve

J. Biol. Chem. published online April 4, 2019
